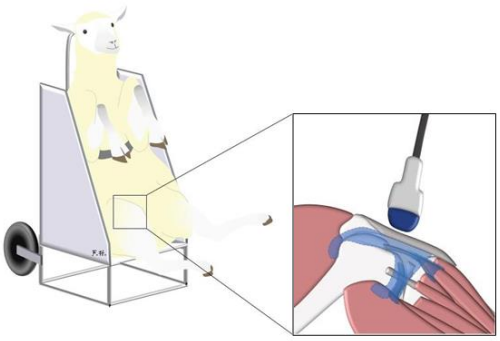

Figure 1: Study conducted with the sheep in a sitting position, hold by an abdominal strap in a dedicated chair.

2.3. 2D Ultrasound

US examination included the evaluation of the entire patellar tendon, the patellar and tibial tuberosity attachments, the adjacent cranial soft tissues and the patellar fat pad using a L3- 12A and LA4-18B linear-array transducer. Tendon echogenicity and homogeneity were assessed in transverse and longitudinal planes. Abnormalities were searched and recorded if present.

2.4. Color doppler ultrasound

Potential neovascularization, that could be a sign of tendon disorder, was assessed by CDUS, using the LA4-18B linear-array transducer, in transverse and longitudinal planes. The entire patellar tendon and the adjacent soft tissues were explored.

2.5. Shear wave elastography

2D ultrasound was used to locate the patellar tendon and align the transducer longitudinally with the tendon fibers. When a correct image of the patellar tendon, without artefacts, was obtained, the shear wave mode was activated to obtain a color-coded elastogram. Through a dual display, the fiber-transducer alignment was constantly verified. The size of the rectangular acquisition box was defined previously to the data acquisition, to maximize the amount of tissue analyzed, avoiding the tendon extremities. The diameter of the circular ROI (Region of Interest) was held constant at 0.3 cm throughout the measurements in all the limbs. The ROI was set manually and was centered on the targeted patellar tendon. SWE was assessed in a longitudinal plane, parallel to the fiber orientation, with light pressure on the skin, basically in the mid portion of the tendon, avoiding the tendon extremities, using a LA2-9A linear-array transducer. The transducer was kept motionless during 8-12 seconds to acquire the color-coded elastogram. When the color in the color- coded elastogram was uniform, the image was frozen enabling an off-line analysis through the captured images (Figure 2). Three images were captured, with 6 measurements on each. For each PT, the SWV was assessed, expressed in m/s, as well as the shear elastic modulus expressed in kPa. In our study, we considered the SWV for correlations.

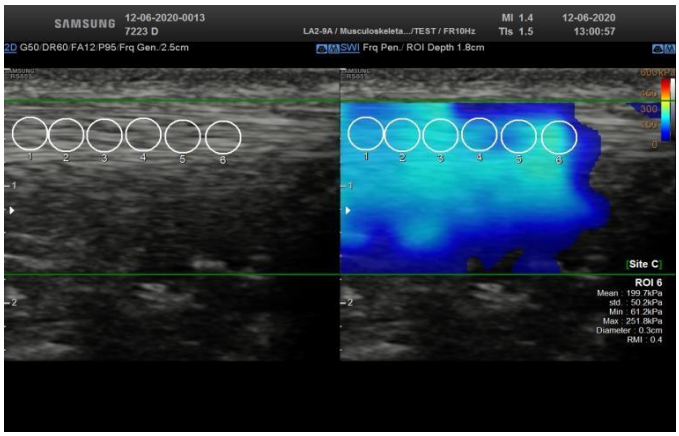

Figure 2: Dual display (left) showing a 2D ultrasound image used to locate the patellar tendon and align the tendon fibers longitudinally with the transducer. When a correct image of the patellar tendon was obtained (right), the shear wave mode was activated to obtain a color-coded elastogram. Three images were captured, with 6 measurements on each.

2.6. Gross anatomy

Animals were sacrificed by intravenous administration of pentobarbital (150 mg/kg). Both hind limbs were transected at the level of the mid-femur, immediately after death. The patellar tendon and its attachments on the patella and the tibial tuberosity were carefully dissected. The patella and tibial tuberosity were sawed at 1.5 cm from their tendon attachment in order to not affect the tendon insertion areas that are fundamental for transferring loads. Each harvested specimen consisting of an intact "patella-patellar tendon-tibial tuberosity" unit was individually wrapped in moistened gauze (with 0.9 % w/v NaCl), sealed in plastic bags, individually identified by a number and stored at -20°C until processed for biomechanical tests.

2.7. Biomechanical tests

All specimens were submitted to biomechanical tests on a same day. In six matched pairs of limbs (n=12), a uniaxial tensile test was performed on patellar tendons following a procedure described previously [20]. The frozen "patella-patellar tendon- proximal tibial" units were thawed to room temperature, cleaned thoroughly with 0.9 % w/v of NaCl solution and placed on a metal frame. The osseous parts of the specimen were cut with pliers to fit the clamp size (Figure 3). The camera was set to 100 fps. Force outputs were obtained via a dedicated 1 kN load cell (Lloyd Instruments Ltd). A series of 10 preconditioning stress-relaxation procedures were performed to obtain a good alignment of fibers prior to tensile testing since tendons had been previously manipulated and then stored at -20°C. As suggested in the ASTM D638 standard [21], the tensile test was performed with a crosshead speed of 5 mm/min. The axial force was recorded and paired with the relative displacement during the tests. The tensile test was performed until failure. The resulting force-displacement curve was analyzed. The linear region of the curve, corresponding to the elastic region, i.e., the elongation of the helical structure of collagen [22], was determined thanks to a dedicated software: a linear fitting process was used to determine the boundaries of the linear region and this latter was studied to obtain the relative stiffness of the tissue

(obtained from the slope of the curve in the selected region). Tendon stiffness, expressed in N/mm, is defined as the ratio between the force applied on the tendon and the change of the tendon length.

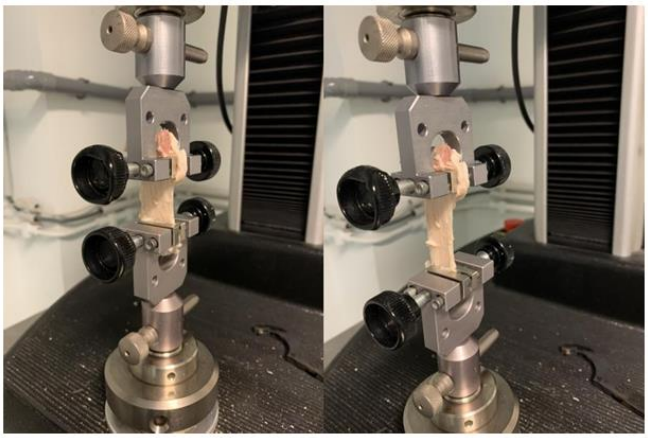

Figure 3: Patella-patellar tendon-tibial tuberosity unit fixed by two clamps. A: at the beginning of the uniaxial tensile test. B: at a more advanced phase of the uniaxial tensile test.

3. Statistical Analysis

Kolmogorov-Smirnov and Shapiro-Wilk tests were used to examine the normality of data (stiffness). Due to the normality of data, parametric tests were used. The Paired T test was used to compare observations that were not independent (difference in stiffness between left and right hindlimbs). Since there was no difference, one limb was randomly chosen within each pair and data obtained from that limb (SWV, tendon stiffness) was used for analysis. Correlations between mechanically measured SWV and tendon stiffness and age were assessed by Pearson correlation coefficient. Data were collected in Microsoft Excel and were analysed using Graph Pad Prism 8. A p-value less than 0.05 was considered to indicate a statistically significant difference.

4. Results

On ultrasound all tendons presented a homogeneous fibrillar structure. We noted no focal or global abnormal thickening. We found no abnormalities in the patellar and tibial tuberosity attachments. The cranial soft tissues adjacent to the patellar tendon and the patellar fat pad were homogeneous in all cases. No neovascularization was observed by CDUS nor in the patellar tendon neither in the adjacent soft tissues. The mean stiffness value of the 12 tendons was 45.69 N/mm (SD+/- 14.56). The tendon stiffness increased until failure. Since there was no difference in patellar tendon stiffness between left and right hindlimbs, one limb was randomly chosen within each pair and data obtained from that limb (Tendon stiffness) was used for analysis. Our tests confirmed that the patellar tendon had a typical non-linear behavior (Figure 4).

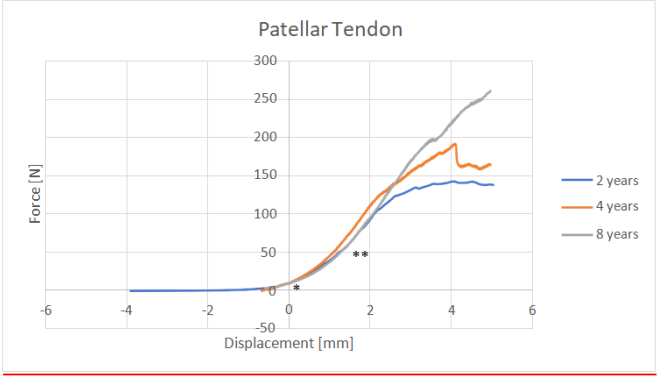

Figure 4: Force-Displacement curve in three different legs showing the initial toe region (*) and the linear region (**).

On SWE, the mean SWV value within the ROI was 6.27 m/s (SD+/-0.6).

We found a statistically not significant positive correlation between SWV and age (r=0.137, p=0.79).

Our data showed a significant positive correlation (r=0.87; p=0.02) between stiffness and SWV (Figure 5).

Correlation between shear wave velocity and stiffness

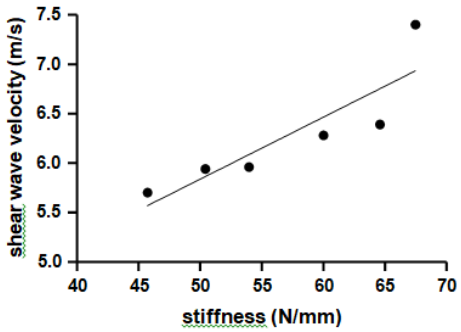

Figure 5: Correlation plot between shear wave velocity (m/s) and stiffness (N/mm). Correlation was significantly positive between shear wave velocity and stiffness.

5. Discussion

In this study the mean stiffness of patellar tendons was 45.69 N/mm (SD+/- 14.56). As previous studies were conducted in other animal models and reported only Young's modulus, our data constitute, to the best of our knowledge, the first reference values for patellar tendon stiffness in sheep. With soft tissue structures, as they are quite irregular, the estimation of the cross-sectional area during the test may be quite difficult and could induce some measure errors in the determination of the stress (ratio between the force applied and the cross-sectional area) and therefore of the Elastic Modulus. For that reason, we decided to measure the stiffness as our technique is

elastography and MyotonPRO. Scientific Reports 8 (2018): 17064.

Hsiao YY, Yang TH, Chen PY, et al. Characterization of the extensor digitorum communis tendon using high-frequency ultrasound shear wave elastography. Medical Physics 47 (2020): 1609-1618.

Martin JA, Biedrzycki AH, Lee KS, et al. *In vivo* measures of shear wave speed as a predictor of tendon elasticity and strength. Ultrasound in Medicine & Biology 41 (2015): 2722-2710.

32. Rosskopf AB, Bachmann E, Snedeker JG, et al. Comparison of shear wave velocity measurements assessed with two different ultrasound systems in an *ex-vivo* tendon strain phantom. Skeletal Radiology 45 (2016): 1541-1551.
33. Hardy A, Rodaix C, Vergari C, et al. Normal range of patellar tendon elasticity using the sharewave elastography technique: an *in vivo* study in normal volunteers. Surgical Technology International 31 (2017): 227-230.

Kuervers EJ, Firminger CR, Edwards WB. Effect of knee angle and Quadriceps muscle force on Shear-Wave Elastography measurements at the Patellar Tendon. Ultrasound in Medicine & Biology 47 (2021): 2167-2175.

35. Yu M, Wu J, Hou J, et al. Young's Modulus of Bilateral Infraspinatus Tendon Measured in Different Postures by Shear Wave Elastography Before and After Exercise. Journal of Orthopaedic Surgery 13 (2021): 1570–1578.
36. Zhang ZJ, Ng GYF, Fu SN. Effects of habitual loading on patellar tendon mechanical and morphological properties in basketball and volleyball players. European Journal of Applied Physiology 115 (2015): 2263-2269.
37. Mannarino P, Lima KMM, Fontenelle CRC, et al. Analysis of the correlation between knee extension torque and patellar tendon elastic property. Clinical Physiology and Functional Imaging 38 (2018): 378-383.
38. Chiu YH, Chang KV, Chen IJ, et al. Utility of sonoelastography for the evaluation of rotator cuff tendon and pertinent disorders: a systematic review and meta-analysis. European Radiology 30 (2020): 6663-6672.